Journal of Multidisciplinary Engineering Science and Technology (JMEST)
ISSN: 2458-9403
Vol. 7 Issue 3, March - 2020

Synthesis of AlFeCrNiV high entropy alloy by gas atomization and selective laser melting

Yuyang Liao, Pengfei Zhu, Song Li
State Key Laboratory for Powder Metallurgy,
Central South University, Changsha 410083, China
E-mail address: ls2011sl@csu.edu.cn

***Abstract*—The $Al_{0.5}FeCrNi_{2.5}V_{0.2}$ high-entropy alloy (HEA) powders were successfully obtained by gas atomization. The gas-atomized alloy particles possessed a single face-centered cubic (FCC) phase and exhibited nearly-spherical shapes with relatively smooth surfaces. The gas-atomized HEA powders with the median diameter (Dv50) of 12.8 μm were used as the feedstock powders for the subsequent selective laser melting (SLM) process. The microstructure, densification and microhardness of the as-built HEAs were investigated by varying the laser power and scanning speed.**

Keywords—High entropy alloy; Gas atomization; Selective laser melting; Densification; Microhardness

I. INTRODUCTION

As a new class of advanced alloys, high entropy alloys (HEAs) have gained more and more attentions because of their unique microstructure and excellent combined propertied such as high strength and ductility [1-3]. Compared with conventional alloys, HEAs are generally designed on five or more principle elements in equimolar or near-equimolar ratios with high configurational entropy of mixing due to the mutual solubility of constituent elements. According to the high entropy effect and Gibbs rule, HEAs tend to form simple solid solution rather than intermetallic compounds [3, 4]. At present, HEAs are mainly produced by casting method and mechanical alloying combined with subsequent consolidation process [5-7]. The conventional casting technique easily induces some structural defects in HEAs containing multiple elements, such as compositional segregation, voids and porosity [8, 9], and has the disadvantages in terms of cost and efficiency, especially when the complex geometry is required. The HEA powders obtained by mechanical alloying possess a fine or nanocrystalline microstructure with compositional homogeneity, but they are easily contaminated by milling media and atmosphere due to the long high-energy milling process. Therefore, it is very necessary to develop novel manufacturing methods for HEAs. Recently, Additive manufacturing of HEAs has gained increasing attention due to its advantages including unrivalled design freedom, near net-shape forming, efficient material usage and high solidification rates [10-12]. However, it is well known that the surface quality, densification and mechanical properties of the final HEA parts obtained by additive manufacturing are closely linked with the quality of feedstock powders [13]. Mechanical alloying can be used for the preparation of HEA powders, but the powders with irregular shape induced by mechanical alloying are not suitable for additive manufacturing process because it increases the flow time and possibly reduces the packing density [14]. Gas atomization is an alternative way to produce HEA powders with spherical shape for additive manufacturing [15, 16]. The powders prepared by gas atomization are of higher purity and more homogeneous both in the composition and the morphology compared with mechanical alloying.

Based on the above background, in this work, the gas atomization method was used for the fabrication of the precipitation-hardening $Al_{0.5}FeCrNi_{2.5}V_{0.2}$ HEA powders. The as-received HEA powders were chosen as the feedstock powders used for the subsequent additive manufacturing process, selective laser melting (SLM). The surface morphology, particle size distribution and chemical composition homogeneity of the gas-atomized powders were investigated in details. The microstructure, densification and microhardness of the as-built HEA by SLM were examined.

II. EXPERIMENTAL PROCEDURES

The $Al_{0.5}FeCrNi_{2.5}V_{0.2}$ HEA powders of Al, Fe, Cr, Ni, and V with high purity were prepared by gas atomization process, which was carried out under the protection of argon atmosphere to avoid oxidation. The SLM processing of the gas-atomized $Al_{0.5}FeCrNi_{2.5}V_{0.2}$ HEA powders was performed on a FS271 M machine (Farsoon, Inc, China), equipped with a maximum laser power of 500 W and a nominal focused laser spot diameter of 90 μm. During the SLM process, the laser scanning direction was rotated by 67° between adjacent layers. The hatch space is set to be 80 μm and the layer thickness is 50 μm. The effects of the processing parameters on the densification and microhardness of the HEAs obtained by SLM were explored by varying the laser power and scanning speed. The related parameters of six representative SLM-processed groups were listed in Table 1. The volumetric energy density (VED) corresponding to each parameter group was determined according to the formula [16].

A Malvern MICRO-PLUS (Malvern Panalytical, UK) laser diffraction particle size analyzer was used to measure the particle size distribution of the powder. Phase identification was carried out by an X-ray diffractometer (XRD, Rigaku D/MAX2550). The microstructure of the as-prepared powder and bulk

samples was characterized under a VEGA3-SBH (Tescan, Czech Republic) scanning electron microscope (SEM) equipped with an energy dispersive X-ray analysis system. The Archimedean method was utilized to determine the density of bulk samples obtained by SLM. The hardness values of the as-built HEAs were tested using a HV-1000Z Vickers hardness tester with a load of 200 g and a holding time of 15 s. At least 10 measurements were performed at different areas for each sample.

Table 1 Processing Parameters of SLM process

Processing parameter	A	B	C	D	E	F
Laser power (W)	200	300	200	300	200	300
Scanning speed (mm/s)	1000	1000	800	800	600	600
Volumetric energy density (J/mm^3)	50	75	62.5	93.75	83.3	125

III. Results and Discussion

Figure 1 shows the SEM images and EDX analysis of the as-received $Al_{0.5}FeCrNi_{2.5}V_{0.2}$ HEA powders obtained by gas-atomization. As shown in Fig. 1(a), most of powders exhibit a spherical morphology. Otherwise, some small satellite particles, which are typically several microns in size, are also found to adhere to the larger particles due to the turbulent flow in the atomization chamber and the collisions of the solidifying droplets [17]. The EDX line scanning data of cross-section of the as-received HEA powder shown in Fig. 1(b) confirms that the overall composition of the gas-atomized alloy powder is homogeneous and close to its nominal composition. A dendritic solidification microstructure is clearly revealed and grain boundaries can be observed on particle surfaces according to the SEM image of the cross-section microstructure presented in Fig. 1(b).

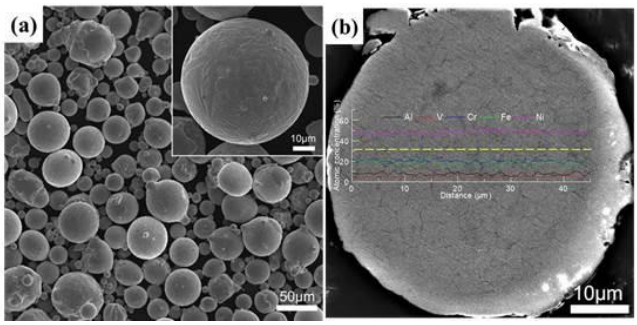

Figure 1 SEM images and EDX analysis of the gas-atomized $Al_{0.5}FeCrNi_{2.5}V_{0.2}$ HEA powders

The particle size distributions of the as-received HEA powders obtained by gas-atomization are shown in Fig. 2. The relatively broad size distribution range for the gas-atomized powders can be seen in Fig. 2(a). The median diameter (Dv50) of the alloy powders is 41.8 μm and the yield of fine powder (no more than 70 μm) is about 90%, indicating that the high yield of fine powder is gained. However, the gas-atomized powders with the broad powder size distribution range are not suitable for the SLM process [18]. Therefore, the relatively narrow particle size distribution of the as-received HEA powders was obtained after the further sieving process. The corresponding particle size distribution curve is shown in Fig. 2(b). The median diameter (Dv50) of the powders further decreases to 12.8 μm and the yield of fine powder (no more than 20 μm) is above 80%. Otherwise, the particle size distribution overlap can be also found in Fig. 2 because the sieving process is not perfect, for example, plugged mesh by spherical powder. The XRD pattern of the gas-atomized HEA powders is shown in Fig. 3. Only one set of diffraction peaks corresponding to a single face centered cubic (FCC) phase can be seen.

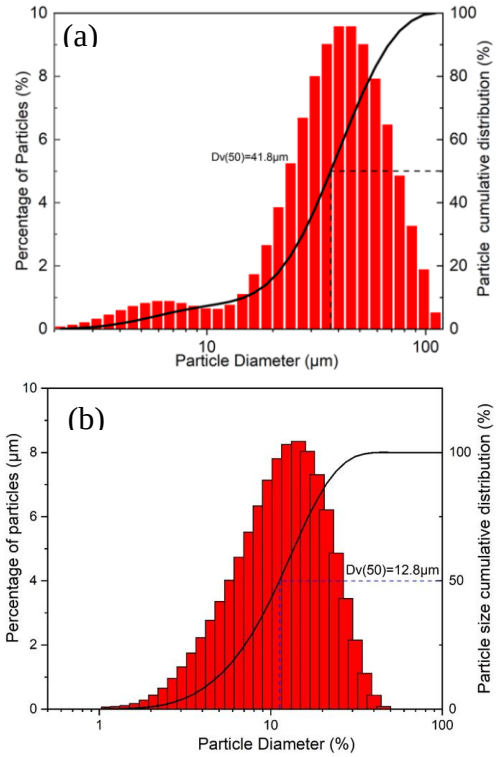

Figure 2 Particle size distributions of the as-received HEA powders obtained by gas-atomization

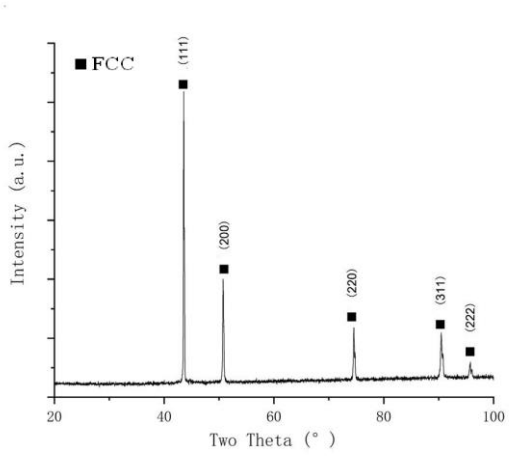

Figure 3 XRD pattern of the gas-atomized HEA powders

The gas-atomized HEA powders with the median diameter (Dv50) of 12.8 μm were selected as the feedstock powders for the SLM process. Figure 4(a) shows the appearances of as-built $Al_{0.5}FeCrNi_{2.5}V_{0.2}$ HEAs obtained by SLM. After printing, there are not obviously visible cracking and delamination on the surfaces of the as-built specimens, but different extent of swelling and fusion can be found. The effect of laser power and scanning speed on the densification of the as-built HEA by SLM were systematically investigated by varying these two parameters. Figure 4(b) presents the effects of VED on the density of the as-built HEA obtained by SLM. The density is varied in the range from 7.56 to 7.59 g/mm3 by changing laser power and scanning speed. The highest density of the as-built HEA can be obtained when the VED is 75 and 125 J/mm3, respectively. Regardless of scanning speed, a laser power of 300 W provides higher density of the specimens.

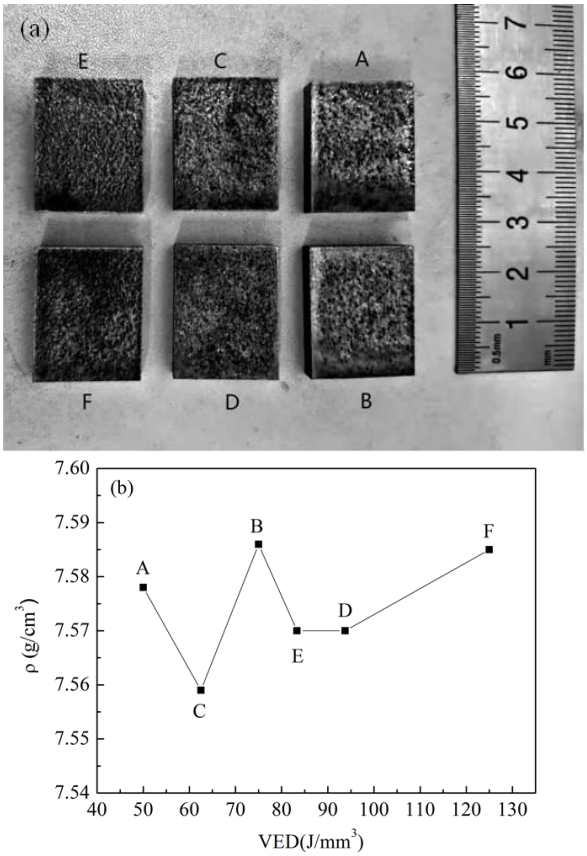

Figure 4 (a) Appearances of as-built $Al_{0.5}FeCrNi_{2.5}V_{0.2}$ HEAs obtained by SLM; (b) Effect of VED on the density of the as-built HEA

Figure 5 shows the SEM images of the transverse sections of the as-built HEAs perpendicular to the building direction. It can be seen that many cracks and pores are presented in all the SLM-processed samples regardless of laser power and scanning speed. The formation of thermal cracks can be ascribed to high thermal stress generated during the SLM process. The formation of hot cracks can be ascribed to high thermal stress generated during the SLM process. The formation of pores and micro-voids is closely related with gas entrapment induced by the turbulent flow in molten pool and the inhibition of the escape of gas from the molten pool by high cooling rate during the SLM process. Figure 6 shows the microhardness of transverse and longitudinal sections of the as-built HEAs obtained by SLM. Whether on the longitudinal or transverse section, the microhardness does not change significantly with the increase of VED. This suggests that the laser VED does not seem to have direct effect on the microhardness of the HEA obtained by SLM. Otherwise, the average microhardness values of transverse section are in the range from 220 to 240 HV, slightly lower than the corresponding longitudinal one. This difference of the microhardness between the transverse and longitudinal section might result from the intrinsic anisotropy induced by the SLM process.

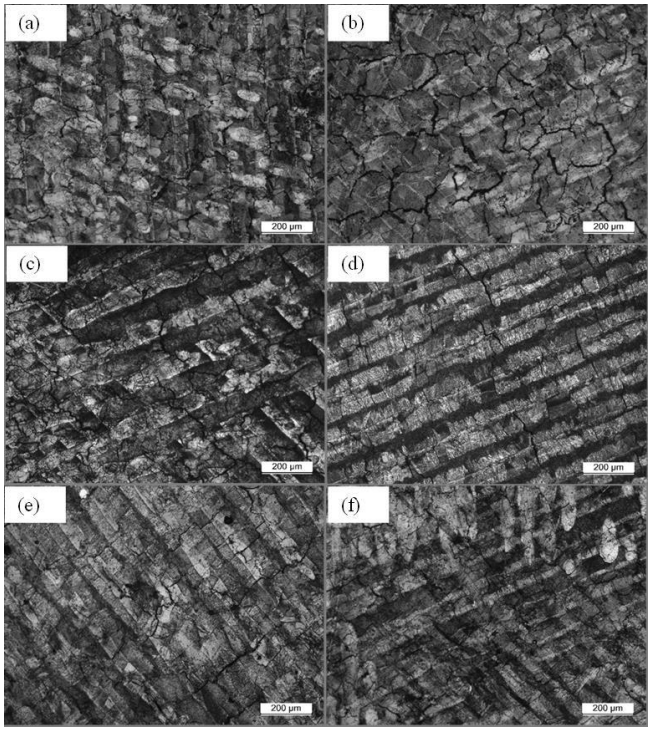

Figure 5 SEM images of the transverse sections of the as-built HEAs perpendicular to the building direction; (a) A; (b) B; (c) C; (d) D; (e) E; (f) F

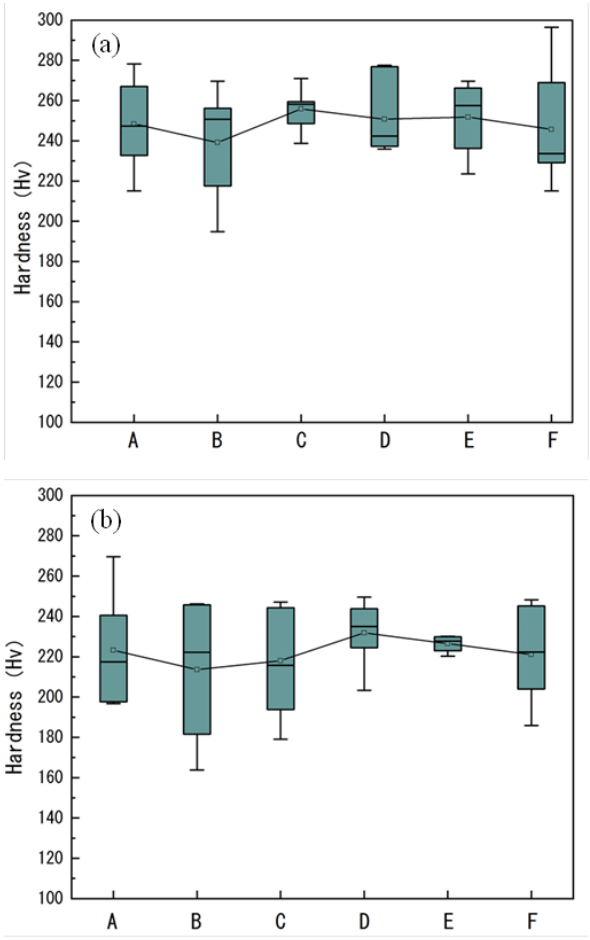

Figure 6 Microhardness of transverse and longitudinal sections of the as-built HEAs obtained by SLM; (a) Longitudinal section; (b) Transverse section

IV. Conclusion

In summary, $Al_{0.5}FeCrNi_{2.5}V_{0.2}$ HEA powders were successfully obtained by gas atomization. A single FCC structure can be found for the as-received powder. Most of the gas-atomized HEA powders are nearly spherical in shape with a homogeneous composition. Bulk $Al_{0.5}FeCrNi_{2.5}V_{0.2}$ HEAs were synthesized by SLM using the gas-atomized powders with the median diameter (Dv50) of 12.8 μm as the feedstock powders. Densification of the as-built HEAs obtained by SLM can be enhanced by adjusting laser power and scanning speed. However, it was difficult to print bulk crack- and pore-free HEAs with SLM by using the current processing parameters. Whether on the longitudinal or transverse section, the microhardness of the HEA obtained by SLM does not obviously change with the increase of VED, but the microhardness of the former is slightly higher than that of the later.

Acknowledgment

The work was primarily financial supported by the National Key R&D Program of China (Grant No. SQ2017YFE030085), State Key Laboratory for Powder Metallurgy and Open sharing Fund for the Large-scale Instruments and Equipments for Central South University.

References

[1] Z. Li, K. G. Pradeep, Y. Deng, D. Raabe, C. C. Tasan, Nature, 2016, 534, 227-230.
[2] J. W. Yeh, S. K. Chen, S. J. Lin, J. Y. Gan, T. S. Chin, T. T. Shun, C. H. Tsau, S. Y. Chang, Adv. Eng. Mater., 2004, 6, 299-303.
[3] [3]Y. Zhang, T. T. Zuo, Z. Tang, M. C. Gao, K. A. Dahmen, P. K. Liaw, Z. P. Lu, Prog. Mater. Sci., 2014, 61, 1-93.
[4] A. L. Greer, Nature, 1993, 366, 303-304.
[5] S. Singh, N. Wanderka, B. S. Murty, U. Glatzel, J. Banhart, Acta Mater., 2011, 59, 182-190
[6] Z. Fu, W. Chen, H. Xiao, L. Zhou, D. Zhu, S. Yang, Mater. Des., 2013, 44, 535-539.
[7] Y. Liu, J. S. Wang, Q. H. Fang, B. Liu, Y. Wu, S. Q. Chen, Intermetallics, 2016, 68, 16-22.
[8] K. G. Pradeep, N. Wanderka, P. Choi, J. Banhart, B.S. Murty, D. Raabe, Acta Mater., 2013, 61, 4696-4706.
[9] C. C. Yang, J. H. Chau, C. J. Weng, C. S. Chen, Y. H. Chou, Mater. Chem. Phys. 2017, 202, 151-158.
[10] H. Attar, S. Ehtemam-Haghighi, D. Kent, M. Dargusch, Int. J. Mach. Tool Manu., 2018, 133, 85-102.
[11] Y. Kok, X. P. Tan, P. Wang, M. L. S. Nai, N. H. Loh, E. Liu, S. B. Tor, Mater. Des., 2018, 139, 565-586.
[12] R. D. Li, P. D. Niu, T. C. Yuan, P. Cao, C. Chen, K. C. Zhou, J. Alloys Compd., 2018, 746, 125-134.
[13] R. Wang, K. Zhang, C. Davies, X.H. Wu, J. Alloys Compd., 2017, 694, 971-981.
[14] V. Manakari, G. Parande, M. Gupta, Metals, 2017, 7, 2-35.
[15] P. P. Ding, A. Q. Mao, X. Zhang, X. Jin, B. Wang, M. Liu, X. L. Gu, J. Alloys Compd., 2017, 721, 609-614.
[16] Y. Brif, M. Thomas, I. Todd, Scr. Mater., 2015, 99, 93-96.
[17] K. W. Wei, Z. M. Wang, F. Z. Li, H. Zhang, X. Y. Zeng, J. Alloys Compd., 2019, 774, 1024-1035.
[18] I. Kunce, M. Polanski, K. Karczewski, T. Plocinski, K.J. KurzydlowskiMi, J. Alloys Compd., 2015, 648, 751-758.
[19] I. E. Anderson, E. M. H. White, R. Dehoff, Curr. Opin. Solid. State. Mater. Sci., 2018, 22(1), 8-15.
[20] P. D. Niu, R. D. Li, S. Y. Zhu, M. B. Wang, C. Chen, T. C. Yuan, Opt. Laser. Technol. 2020, 127, 106147 [1] J. Banhart, Prog. Mater. Sci. 2001, 46(6), 559-632.